



**HAL**  
open science

## Degradable double hydrophilic block copolymers and tripartite polyionic complex micelles thereof for small interfering ribonucleic acids (siRNA) delivery

Ayman El Jundi, Marie Morille, Nadir Bettache, Audrey Bethry, Jade Berthelot, Jérémy Salvador, Sylvie Hunger, Youssef Bakkour, Emmanuel Belamie, Benjamin Nottelet

### ► To cite this version:

Ayman El Jundi, Marie Morille, Nadir Bettache, Audrey Bethry, Jade Berthelot, et al.. Degradable double hydrophilic block copolymers and tripartite polyionic complex micelles thereof for small interfering ribonucleic acids (siRNA) delivery. *Journal of Colloid and Interface Science*, 2020, 580, pp.449-459. 10.1016/j.jcis.2020.07.057 . hal-03025049

**HAL Id: hal-03025049**

<https://hal.umontpellier.fr/hal-03025049v1>

Submitted on 22 Aug 2022

**HAL** is a multi-disciplinary open access archive for the deposit and dissemination of scientific research documents, whether they are published or not. The documents may come from teaching and research institutions in France or abroad, or from public or private research centers.

L'archive ouverte pluridisciplinaire **HAL**, est destinée au dépôt et à la diffusion de documents scientifiques de niveau recherche, publiés ou non, émanant des établissements d'enseignement et de recherche français ou étrangers, des laboratoires publics ou privés.



Distributed under a Creative Commons Attribution - NonCommercial 4.0 International License

# **Degradable double hydrophilic block copolymers and tripartite polyionic complex micelles thereof for small interfering ribonucleic acids (siRNA) delivery**

**Ayman El Jundi,<sup>a,b</sup> Marie Morille,<sup>c\*</sup> Nadir Bettache,<sup>a</sup> Audrey Bethry,<sup>a</sup> Jade Berthelot,<sup>c,d</sup> Jeremy Salvador,<sup>c,e</sup> Sylvie Hunger,<sup>a</sup> Youssef Bakkour,<sup>b</sup> Emmanuel Belamie,<sup>c,d</sup> Benjamin Nottelet<sup>a\*</sup>**

<sup>a</sup> IBMM, Univ Montpellier, CNRS, ENSCM, Montpellier, France

<sup>b</sup> Laboratory of Applied Chemistry (LAC), Faculty of Science III, Lebanese University, P.O. Box 826, Tripoli, Lebanon

<sup>c</sup> ICGM-MACS, Univ Montpellier, CNRS, ENSCM, Montpellier, France

<sup>d</sup> EPHE, PSL Research University, 75014, Paris, France.

<sup>e</sup> Univ Montpellier, CHU Montpellier, INSERM, IRMB, Montpellier, France.

\*Correspondence: M.M: [marie.morille@umontpellier.fr](mailto:marie.morille@umontpellier.fr)

B.N: [benjamin.nottelet@umontpellier.fr](mailto:benjamin.nottelet@umontpellier.fr)

**Abstract:** Polymer vectors for gene therapy have been largely investigated as an alternative to viral vectors. In particular, double hydrophilic block copolymers (DHBCs) have shown potential in this domain, but to date studies mainly focus on non-degradable copolymers, which may be a restriction for further development. To overcome this limitation, we synthesized a DHBC (PEG<sub>43</sub>-*b*-PCL<sub>12</sub>(COOH)<sub>6.5</sub>) composed of a poly(ethylene glycol) (PEG) non-ionic and bioeliminable block and a degradable carboxylic acid-functionalized poly( $\epsilon$ -caprolactone) (PCL) block. The potential of this DHBC as an original vector for small interfering ribonucleic acids (siRNA) to formulate tripartite polyionic complex (PIC) micelles with poly(lysine) (PLL) was evaluated. We first studied the impact of the charge ratio (R) on the size and the zeta potential of the resulting micelles. With a charge ratio R=1, one formulation with optimized physico-chemical properties showed the ability to complex 75 % of siRNA. We showed a stability of the micelles at pH 7.4 and a disruption at pH 5, which allowed a pH-triggered siRNA release and proved the pH-stimuli responsive character of the tripartite micelles. In addition, the tripartite PIC micelles were shown to be non-cytotoxic below 40  $\mu$ g/mL. The potential of these siRNA vectors was further evaluated *in vitro*: it was found that the tripartite PIC micelles allowed siRNA internalization to be 3 times higher than PLL polyplexes in murine mesenchymal stem cells, and were able to transfect human breast cancer cells. Overall, this set of data pre-validates the use of degradable DHBC as non-viral vectors for the encapsulation and the controlled release of siRNA, which may therefore constitute a sound alternative to non-degradable and/or cytotoxic polycationic vectors.

**Keywords:** Degradable double hydrophilic block copolymers, tripartite polyion complex micelles (PIC), pH sensitive micelles, functional poly( $\epsilon$ -caprolactone), gene therapy, siRNA, mesenchymal stem cells, cancer cells.

## 1. Introduction

The ability of small interfering ribonucleic acids (siRNA) to selectively silence gene expression *in vivo* is the cornerstone of numerous recent therapeutic breakthroughs, with the first approved RNA interference therapeutics brought to the market by Alnylam® Pharmaceuticals in 2018 with ONPATRO® (patisiran, to treat hereditary ATTR amyloidosis) and in 2019 with GIVLAARI® (givosiran, to treat acute hepatic porphyria). This success demonstrates the high potential of siRNA-based therapeutics that are currently investigated to treat other disease like cancers (breast, lung, colorectal etc.) or in regenerative medicine and tissue engineering of various tissues (bones, nerves etc.) [1–3]. The outcome of these therapies strongly depends on the ability of the selected formulations to protect siRNA from enzymatic degradation, renal clearance and phagocytosis, but also to deliver their payload in the cytoplasm thanks to an efficient internalization and endosomal escape. To a large extent, viral vectors represent the most effective option for the transduction of cells *in vitro* [4,5]. However, the concern of safety and the high production cost associated with viral vectors strongly impede their transfer to clinical routine [6]. Therefore, non-viral vectors represent a convincing alternative despite their recognized lower transfection efficiency compared to their viral counterparts [7]. Moreover, synthetic vectors offer quasi-infinite possibilities of structural and chemical modulations to improve their efficiency to deliver NA in response to specific triggers.

Among non-viral vectors, Lipofectamine 2000® is a commercial lipidic vector used for *in vitro* studies that demonstrated high siRNA transfection efficiencies in cancer cells [8,9]. Interestingly, it is also considered the most effective vector in MSC with up to 98 % green fluorescent protein (GFP) knockdown efficiency reported in human MSC [10,11]. However, these findings must be balanced with the cytotoxicity associated with this vector [12,13]. Other synthetic transfection systems include mainly cationic polymeric vectors such as

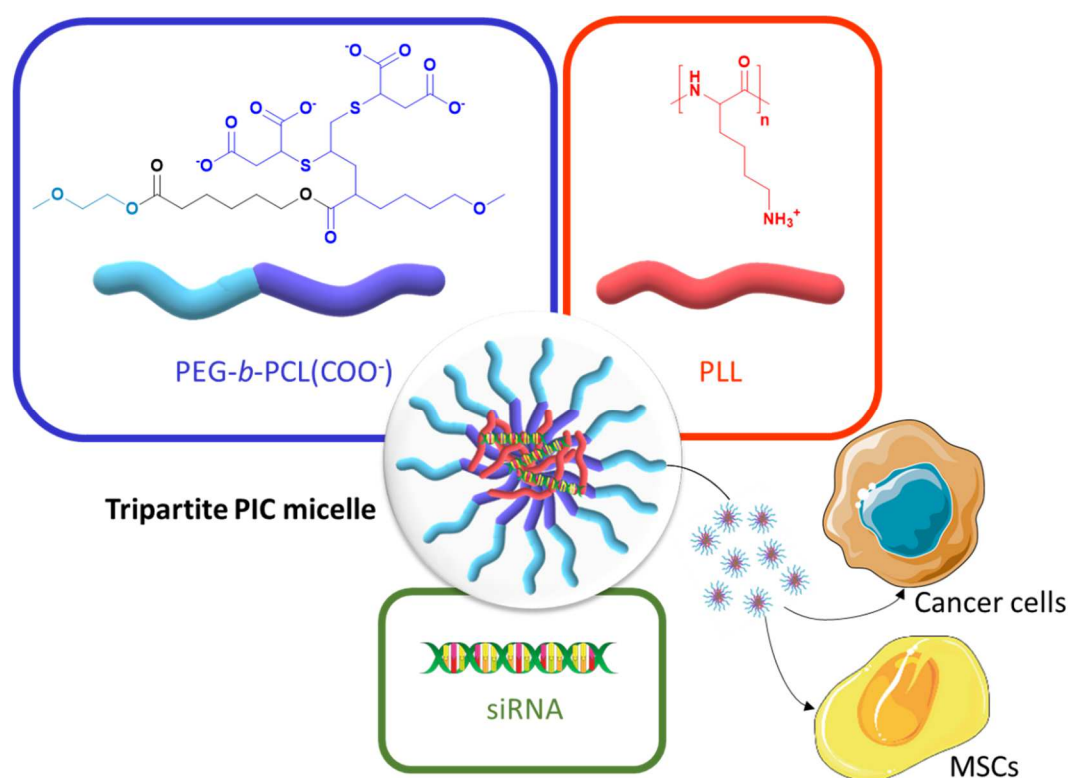
commercial polyethyleneimine (PEI) (ExGen®, in vivo jet-PEI®, etc.) [14], poly-L-lysine (PLL) [15], or poly(amido-amine) (PAMAM) dendrimers [16], which form the so-called polyplexes upon complexation with NA. But these polymeric vectors are of limited interest for clinical application due to their associated cytotoxicity. To circumvent these drawbacks, polyester based systems have been developed to deliver small interfering ribonucleic acid (siRNA) due to their degradability and their long track record in conventional drug delivery [17]. Aliphatic polyester blocks (*eg.* poly(lactide), poly(lactide-*co*-glycolide) or poly( $\epsilon$ -caprolactone) (PCL)) associated or not with cationic polymers (*eg.* PEI, poly(2-dimethylaminoethyl methacrylate)) or cationic polypeptides (*eg.* PLL, poly(arginine)) were proposed [18,19]. However, these hydrophobic polymers, when complexed with NA, generally led to a (highly) positively charged complex, which tends to aggregate and form high sized complexes poorly adapted to an *in vivo* use, and often cytotoxic *in vitro* [20].

Double-hydrophilic block copolymers (DHBC) constitute an interesting alternative class of copolymers to design polymeric vectors for NA delivery with low cytotoxicity. DHBC consist of two or more water-soluble blocks of different chemical nature. A first ionic block, like PEI can complex NA, while a second non-ionic block, generally poly(ethyleneglycol) (PEG), can form an outer shell that stabilizes the polyplex and decreases the overall cytotoxicity of the construct by masking the remaining charges [21]. One advantage of such DHBCs is their ability to form siRNA loaded tripartite polyionic complex (PIC) micelles. Tripartite PIC micelles result from the spontaneous formation of an electrostatic complex between the polyanionic block of the DHBC and the polycation, which forms a liquid precipitate called “coacervate” [22]. The siRNA can then be entrapped in the core of the micelles by complexation with the cationic polymer. Poly(ethyleneglycol)-*b*-poly(methacrylic acid) (PEG-*b*-PMAA) DHBC is a classical example of DHBC used to formulate siRNA tripartite micelles. Examples are reported in the literature with the PEG-*b*-PMAA DHBC being

associated with poly(amido amine) (PAMAM) dendrimers and siRNA for prostate cancer cells transfection [23], or more recently with PLL and siRNA for the transfection of murine MSC (mMSC) [24]. Advantageously, tripartite PIC micelles exhibit a pH sensitivity with a reversible assembly/disassembly. When formulated with weak polyacids, it ensures that siRNA material is released in the acidic pH of the endosomes, which led to efficient gene inhibition and low if any cytotoxicity in the case of selected PEG-*b*-PMAA DHBC / PLL ratios [23–25]. These DHBCs are however not degradable, which is another requirement for biomedical applications. To the best of our knowledge, only two examples of degradable DHBCs have been reported for cell transfection so far and used to form polyplexes by mixing them with plasmid DNA (pDNA). The first one was reported by Zhang *et al.* who developed PEG-*b*-poly(2-(2-aminoethoxy)ethoxy) phosphazene DHBCs able to form polyplexes with a size of ~100 nm and used for the transfection of Hela cancer cells [26]. However, despite high levels of internalization, the transfection efficiencies were limited to 15%. The second example is based on a cationic derivative of poly(aspartamide) (PAsp) bearing N-(2-aminoethyl)-2-aminoethyl (DET) moieties developed by Takae *et al.* [27]. They prepared a reducible PEG-*b*-PAsp(DET) DHBC containing a central disulfide bond and able to form polyplexes of ~80 nm with pDNA. Compared to branched PEI controls, similar transfection levels were obtained with this DHBC in Hela cancer cells, but with a twice lower cytotoxicity.

In the present study, we aim at taking advantage of a degradable DHBC based on functional polyesters to be used for the preparation of degradable tripartite PIC micelles for siRNA delivery to mMSC and cancer cells (Scheme 1). We recently designed a DHBC composed of a bioeliminable PEG block and a degradable PCL block functionalized with multiple pending carboxylic groups. Such anionic DHBCs demonstrated a high potential for drug delivery thanks to their ability to form PIC micelles with cationic drugs, such as the anticancer drug doxorubicin, while their pH-responsiveness ensures a release triggered by

tumoral acidic pH conditions [28]. Based on these results, we investigated in this work the influence of the charge ratio between the anionic DHBC and the counter-polycation PLL on micelles formation and properties. We also studied the ability of the different formulations to stably incorporate siRNA and to disassemble at endosomal acidic pH. We finally assessed the potential of the selected tripartite PIC micelles in terms of cytotoxicity, cellular internalization efficiency, and gene inhibition towards mMSC and human breast cancer cells.



**Scheme 1.** Illustration of the components forming the degradable tripartite PIC micelles and of the cells used to evaluate their potential of transfection.

## 2. Materials and Methods

### 2.1. Chemical and biochemical reactants

$\alpha$ -methoxy, $\omega$ -hydroxyl poly(ethylene glycol) (PEG<sub>2k</sub>, Mn=2000 g/mol), stannous octoate (Sn(Oct)<sub>2</sub>, 92.5-100 %),  $\epsilon$ -caprolactone (CL, 97 %), mercaptosuccinic acid (MSA, 97 %), 2,2-dimethoxy-2-phenyl-acetophenone (DMPA, 99 %), propargyl bromide (PgBr, 80 wt% in

toluene), lithium diisopropylamide (LDA, 97 %, 2 M in THF/heptane/ethylbenzene), were purchased from Sigma-Aldrich (St-Quentin Fallavier, France). THF was dried using a Pure Solv Micro Single Unit (Inert®) system. Toluene was distilled over calcium hydride (CaH<sub>2</sub>). PEG was dried by an azeotropic distillation in dry toluene. CL was dried over CaH<sub>2</sub> for 48 h at room temperature and distilled under reduced pressure. Alexa fluor<sub>488</sub>-tagged siRNA (Alexa<sub>488</sub>-siRNA) and siRNA targeting mouse Runx2 (siGENOME, mix of 4 target sequences: ACAGAGGGCACAAGUUCUA, CGAAAUGCCUCCGCUGUUA, CAAGAAGGCUCUGGCGUUU and CCAUAACAGUCUUCACAAA) were obtained from Dharmacon (France). Poly-L-lysine (PLL) hydrobromide (21 000 g/mol) was obtained from Alamanda Polymers (Huntsville, USA). MTT (3-[4, 5-dimethylthiazol-2-yl]-2, 5-diphenyltetrazolium bromide; thiazolyl blue), methyl-β-cyclodextrin (MβCD), genistein, chlorpromazine and cytochalasin D were obtained from Sigma Aldrich. The siRNA firefly luciferase (siFluc) sequence (sense: 5'-CUUACGCUGAGUACUUCGAdTdT-3' and anti-sense UCGAAGUACUCAGCGUAAGdTdT) was purchased from Eurogentec (Serring, Belgium). Luciferin was purchased from Promega (France).

## 2.2 Characterizations and methods

*NMR spectroscopy.* <sup>1</sup>H NMR (300 MHz) spectra were recorded on a Bruker AMX300 spectrometer at 25 °C. Deuterated chloroform was used as solvent, chemical shifts were expressed in ppm with respect to tetramethylsilane (TMS).

*Molecular weight measurements.* The number-average and weight-average molecular weights (M<sub>n</sub> and M<sub>w</sub>, respectively) and dispersity (Đ, M<sub>w</sub>/M<sub>n</sub>) of the polymers were determined by size exclusion chromatography (SEC) using a Viscotek GPCmax VE2100 liquid chromatograph equipped with a Viscotek VE3580 refractive index detector operating at 35 °C. Tetrahydrofuran was used as the eluent and the flow rate was set up at 1.0 mL/min.



Two LT5000L 300 x 7.8 mm columns operating at 29°C were used. Calibrations were performed with polystyrene standards (600 – 1.10<sup>6</sup> g/mol).

*Ultra-Violet source (UV-source).* Photoirradiation was carried out using DYMAX BlueWave® 200 UV lamp equipped with a waveguide (exit power 6 mW/cm<sup>2</sup>).

### 2.3. Synthesis of PEG-*b*-PCL(COOH) DHBCs

The synthesis of DHBCs composed of a PEG nonionic block and a carboxylic functional PCL anionic block was carried out according to our recent procedure [28]. Detailed procedures and chemical structures (Figure S1) can be found as Supplementary Materials. <sup>1</sup>H NMR analysis of the commercial  $\alpha$ -methoxy, $\omega$ -hydroxyl poly(ethylene glycol) revealed that the exact molecular weight was 1900 g/mol (degree of polymerization DP = 43), to be compared with the 2000 g/mol reported by the supplier. For this reason, the notation PEG<sub>43</sub> is used in the rest of this work. In a first step, amphiphilic PEG-*b*-PCL diblock copolymers were synthesized by ring opening polymerization (ROP) of  $\epsilon$ -caprolactone in toluene at 100°C using PEG<sub>43</sub> and Sn(Oct)<sub>2</sub> as initiator and catalyst, respectively. Propargylation of the resulting PEG<sub>43</sub>-*b*-PCL<sub>15</sub> was performed according to a procedure reported by our group. A first activation of the PCL chain by the removal of a proton of the methylene group in  $\alpha$  position of the ester carbonyl using LDA, followed by reaction with the electrophilic PgBr [28]. In a last step, propargylated PEG<sub>43</sub>-*b*-PCL<sub>12</sub> (PEG-*b*-PCL(YNE)) was functionalized with carboxylic groups via photoradical thiol-yne addition of mercaptosuccinic acid (MSA) according to a modified procedure [28,29]. PEG<sub>43</sub>-*b*-PCL<sub>12</sub>(COOH)<sub>6.5</sub> was obtained with a 65 % yield.

<sup>1</sup>H NMR (300 MHz, CDCl<sub>3</sub>):  $\delta$  = 4.05 (t, CH<sub>2</sub>CH<sub>2</sub>OCO), 3.65 (m, OCH<sub>2</sub>CH<sub>2</sub>O), 3.35 (s, CH<sub>3</sub>O), 3.05-2.40 (m, COCHCH<sub>2</sub>CH<sub>2</sub>, CHCH<sub>2</sub>CHS, SCHCH<sub>2</sub>S, CH<sub>2</sub>COOH), 2.30 (t, COCH<sub>2</sub>CH<sub>2</sub>), 1.85 (m, CHCH<sub>2</sub>CHS, COCHCH<sub>2</sub>CH<sub>2</sub>CH<sub>2</sub>CH<sub>2</sub>O), 1.65 (m, COCH<sub>2</sub>CH<sub>2</sub>CH<sub>2</sub>CH<sub>2</sub>CH<sub>2</sub>O), 1.38 (m, COCH<sub>2</sub>CH<sub>2</sub>CH<sub>2</sub>CH<sub>2</sub>CH<sub>2</sub>O) (Figure S2). SEC: Mn 4600

g/mol,  $\bar{D}$  1.6. Degree of substitution (DS) of MSA groups with respect to CL units 25 % (from NMR analysis). DS of MSA groups with respect to CL units 27.5 % (from carboxylic groups' titration, corresponding to 6.5 carboxylic groups per PCL block).  $M_n$  NMR = 3600 g/mol (1900 g/mol for PEG block and 1700 g/mol for the functionalized PCL(COOH) block)

#### 2.4. Tripartite PIC micelles formulation

Micelles were prepared following the general protocol previously described [30]. For physico-chemical study, micelles were prepared in purified water for zeta potential measurements; whereas for DLS and biological use they were prepared in sterile phosphate buffer saline (PBS). In a typical experiment, an aqueous solution of the polycation (PLL) was prepared at a charge concentration of  $\sim 4.4 \times 10^{-3}$  mol/L (corresponding to 0.92 mg/mL of PLL) (Table S1). SiRNA was added at the desired concentration (1.5 or 3  $\mu$ M) to form the initial complex, and this intermediate mix (solution 1) was incubated for 10 minutes at room temperature. Based on the assumption that a double stranded 20pb siRNA brings 40 negative charges, at a siRNA concentration of 1.5  $\mu$ M, the charge concentration was calculated to be  $6.10^{-5}$  mol/L  $[\text{PO}_3^-]$ . Micelles were then obtained by mixing this solution 1 with the solution 2 containing the polyanionic copolymer of PEG<sub>43</sub>-*b*-PCL<sub>12</sub>(COOH)<sub>6.5</sub>. To obtain a charge ratio of 1 ( $R = ([\text{NH}_3^+] + [\text{NH}_2]) / ([\text{COO}^-] + [\text{COOH}]) = 1$ ), solution 2 was prepared at the appropriate concentration (2.9 mg/mL,  $4.4 \times 10^{-3}$  mol/L of carboxylic groups). When varying the charge ratio from 0.5 to 2, PEG<sub>43</sub>-*b*-PCL<sub>12</sub>(COOH)<sub>6.5</sub> copolymer concentration was fixed while PLL concentration was adjusted (0.46 mg/mL for R=0.5 and 1.84 mg/mL for R=2). Examples of formulations are provided in Table S1. When formulated in water, the pH was adjusted to 7.4 using 0.05 M NaOH. The final mixture was then stirred at 4°C for 12h.

## 2.5. Tripartite PIC micelles characterization

### 2.5.1. *Dynamic light scattering and zeta potential measurements*

Dynamic light scattering (DLS) measurements (NanoZS, Malvern Instruments, UK) were performed with a He–Ne laser (wavelength: 632.8 nm), at a temperature of 25 °C and a scattering angle of 173° for detection. The CONTIN method was utilized for data analysis. Tripartite PIC micelles formulations were filtered through a 0.2 µm poly(tetrafluoroethylene) microfilter before measurements. Hydrodynamic diameters ( $D_h$ , nm) (intensity distribution) were measured in PBS, while zeta potentials (mV) were measured only in milliRO water by laser Doppler electrophoresis. Typical formulations used are provided in Table S1. Polydispersity Index (PDI), relative to the width of the population size dispersion, was also measured. The stability of the micelles, as well as pH-triggered disassembly of micelles in free acidic water, were assessed by measuring the hydrodynamic diameter and scattered light intensity expressed as the Derived Count Rate (DCR, measured in “kcps” (kilo counts per second)). DCR is the raw intensity of light scattered by micelles in suspension, irrespective of the attenuator used. To assess their pH-sensitivity, micelles were prepared as indicated above, their formation assessed by DLS, and one given formulation was then adjusted to pH =5, stirred for 2h, and then measured again with the NanoZS (measures were performed 3 times with n=3).

### 2.5.2. *Nanoparticle tracking analysis*

Nanoparticle tracking analysis (NTA) was performed to investigate the size distribution and morphology of the micelles at 25°C using a NanoSight NS300 (Malvern Instruments, UK). Suspensions were diluted with particle-free Dulbecco’s Phosphates Buffered Saline (DPBS) to obtain a particle concentration in the  $1 \times 10^7$ – $1 \times 10^9$  particles/mL range, as recommended by manufacturer. Measurements were performed with a 405 nm laser. Suspensions were

analyzed using the NanoSight NTA 3.2 software following a tailored script: temperature was set at 25 °C, syringe pump at 40 AU (arbitrary unit), 3 videos of 60 s were recorded. Videos were recorded with a camera level set to 16 and analyzed with a detection threshold set to 6 (measures were performed 3 times with n=3).

### 2.5.3. Encapsulation efficiency

#### a. Qualitative evaluation by electrophoresis

5  $\mu$ L 10pb DNA ladder (Invitrogen, ThermoFisher, molecular weight size marker), 15  $\mu$ L of free siRNA solution (3  $\mu$ M) or siRNA associated to PLL (3  $\mu$ M) or micelles (3  $\mu$ M) formulated in PBS were loaded in a 5 % (w/v) agarose gel associated with ethidium bromide. Electrophoresis was carried out at a constant voltage (100 V) for 30 min in Tris-borate-Ethylenediaminetetraacetic acid (TBE) buffer; then the gel was imaged under UV illumination.

#### b. Quantitative determination by Alexa Fluor<sub>488</sub> fluorescence titration

A spectrofluorophotometer RF-5301PC (Shimadzu) was used to perform Alexa<sub>488</sub> fluorescence measurements with an excitation wavelength of 480 nm (slit width: 5.0 nm) and emission wavelength of 580 nm (slit width: 3.0 nm). The fluorescence of working standard solutions of Alexa<sub>488</sub>-siRNA, diluted or complexed into micelles in PBS at concentrations of 3  $\mu$ M, was determined in a quartz microcuvette (pathlength 3 mm). First, 300  $\mu$ L of each solution were put into ultrafiltration devices (Vivaspin® 500  $\mu$ L tubes from Sartorius (Stedim, France) containing a tangential filtration unit with a 100 000 g/mol molecular weight cut off) and centrifugation was performed at 13, 000 g for 10 min at 4 °C to separate micelles (retentates) from uncomplexed siRNA in solution (filtrate). It should be noted that, 1) because reverse spinning was not possible with the Vivaspin® tubes and 2) due to possible losses on the membrane surface, encapsulation efficiencies were determined indirectly from siRNA

quantities present in the filtrates. For this purpose, the volume of the filtrate was measured and Alexa<sub>488</sub> fluorescence measurements were performed without further preparation. (Measures were performed 3 times with n=3)

## 2.6. Cell culture

Culture medium Dulbecco's modified Eagle's medium (DMEM) and reduced serum medium (optiMEM), trypsin, DPBS, Fetal Bovine Serum (FBS), glutamine (100×), penicillin–streptomycin (PS, 10 000 U/mL) and Lipofectamine 2000<sup>®</sup> were obtained from Life Technologies (USA). Mesenchymal stem cells (designated as mMSC B16-GFP) were isolated by flushing the bone marrow of femurs from C57BL/6-GFP mice. Cell suspension was maintained in complete DMEM (supplemented with 10 % fetal bovine serum, 1 % glutamine and 1 % penicillin/streptomycin, equivalent to final concentrations of 2 nM for glutamine, 100 U mL<sup>-1</sup> for penicillin and 100 µg/mL for streptomycin) at 37 °C, 5% CO<sub>2</sub>, and 100 % humidity until a homogeneous population of cells expressing MSC markers was obtained. Cells were characterized by their phenotype (expression of CD44, Sca-1 and lack of hematopoietic markers CD11b, CD14, CD45) and their ability to differentiate into osteoblasts expressing Runx2, AP and OC, adipocytes expressing PPAR $\gamma$ , LPL, and FABP4 and chondrocytes expressing Type II procollagen variant B Coll2B, Aggrecan, and link protein). The cells were used between passages 16 and 36 [24].

MDA-MB-231-Luc-RFP stable cell line was obtained from AMSBIO (SC041, Abingdon, UK). Cells were grown in phenol red-free F12/Dulbecco's modified Eagle's medium (DMEM) supplemented with 10 % FCS and 0.05 mg mL<sup>-1</sup> gentamycin. Cells were incubated at 37°C in a humidified atmosphere with 5 % CO<sub>2</sub>.

## 2.7. Cytotoxicity

### 2.7.1. Mesenchymal stem cells

5000 mMSC B16-GFP cells in 150  $\mu$ L complete DMEM per well were incubated during 48h in a 96-well assay plate with either PIC micelles PLL/ PEG<sub>43</sub>-*b*-PCL<sub>12</sub>(COOH)<sub>6.5</sub> (DHBC/PLL; 3.82mg/mL) or polymer alone (PEG<sub>43</sub>-*b*-PCL<sub>12</sub>(COOH)<sub>6.5</sub>) (DHBC) at different concentrations (from 0 to 600  $\mu$ g/mL of DHBC/PLL PIC micelles, corresponding to 7.6 to 455  $\mu$ g/mL of DHBC (2.9 mg/mL)) in complete DMEM. A CellTiter 96® AQueous Non-Radioactive Cell Proliferation Assay, obtained from Promega (USA), was used to evaluate the cell viability following the manufacturer's instructions. Absorbance was measured at 490 nm after 4 h of incubation, and the background corresponding to wells free of cells (mean of 3) was subtracted from each triplicate mean.

### 2.7.2. Cancer cells

MTT assay was performed to evaluate the cell death. Briefly, the day prior to transfection, 2000 MDA-MB-231 cells were seeded into a 96 multi-well plate in 200  $\mu$ L complete culture medium. 24h after seeding. The PLL and the DHBC-PLL solutions were added on cells with increasing concentrations (corresponding to concentrations from 0 to 95  $\mu$ g/mL and from 0 to 400  $\mu$ g/mL, respectively, to ensure the comparable concentrations of PLL in both formulations) for 72h at 37°C in a humidified atmosphere with 5 % CO<sub>2</sub>. After this incubation, cells were treated for 4 h with 0.5 mg/mL of MTT in media. The MTT/media solution was then removed and the precipitated crystals were dissolved in ethanol/dimethyl sulfoxide (1:1). The plate was gently rotated on an orbital shaker for 10 min to completely dissolve the precipitate. The absorbance was detected at 540 nm with a Microplate Reader (Multiskan FC, ThermoFisher Scientific, France). Averaged results (n=3) were normalized to non-treated cells (Figure S7).

## 2.8. Flow cytometry analysis

55000 mMSC were seeded in a 12-well assay plate and allowed to adhere for 24 h. Free siRNA solution (3  $\mu$ M), PLL-siRNA (polyplexes) (3  $\mu$ M), and siRNA loaded micelle suspensions (3  $\mu$ M) were then added to have final siRNA concentration of 50 nM per well. After 2h of incubation at 37 °C, 5% CO<sub>2</sub> in a humidified atmosphere, cells were collected using trypsin-ethylenediaminetetraacetic acid, washed twice with DPBS, centrifuged (1800 rpm, 5 min, 4°C) and finally resuspended in Hanks Balanced Saline Solution without Ca<sup>2+</sup>, Mg<sup>2+</sup> before analysis by fluorescence-activated cell sorting (FACS) on a BD Accuri™ C6 Plus (BD Biosciences, USA) (20000 events were counted for each sample). Fluorescence mean values (in the FL1 channel where Alexa 488 fluorescence was observed) were normalized to value of cells incubated with PBS representing 100 %. (Measures were performed 3 times with n=3)

## 2.9. Inhibition of gene expression

### 2.9.1. Mesenchymal stem cells

30,000 mMSC B16-GFP cells were plated in each well of a 24-well assay plate, reaching 70 % confluence after 24h. Blank micelles as well as micelles with 3  $\mu$ M of Runx2-targeting siRNA or siCTL were formulated. Complete medium was subsequently replaced by fresh optiMEM medium and cells were treated with 50 nM of siRNA. Thee control groups were used : untreated cells, cells treated with siRNA Runx2 /Lipofectamine2000® complexes for the positive control, and micelles formulated with a control scramble siRNA (siCTL). Cells were then incubated at 37 °C and 5 % CO<sub>2</sub> in a humidified atmosphere. After 6h, 650  $\mu$ L of DMEM supplemented with 15 % of FBS, 1.5 % of glutamine and 1.5 % of PS were added to reach a final concentration of 10 % FBS, and the cells were incubated again for 48h (n=3).

### 2.9.2. RNA extraction, reverse transcription and real-time quantitative polymerase chain reaction (RT-qPCR)

Total RNA was isolated using a RNeasy mini kit (Qiagen, France) and reverse-transcribed using desoxyribonucleoside triphosphate (dNTP) mix (0.5 mM, Fermentas), Random Hexamer (RH) primer (2.5  $\mu$ M, Fermentas), Dithiothreitol (DTT) 10 mM, 1 $\times$  buffer and Moloney Murine Leukemia Virus (M-MLV) reverse transcriptase (5 U  $\mu$ L<sup>-1</sup>, Invitrogen). Reverse transcription (RT) was performed with a first cycle at 65 °C for 5 minutes and then at 4 °C for 5 minutes for an intermediate mix containing 200pmol of ARN and indicated concentrations of dNTP and RH. Then, DTT, buffer and reverse transcriptase were added at the indicated concentrations, and the mix was subjected to successive incubations at room temperature for 5 min, then at 37 °C for 50 min and finally at 70 °C for 15 min. Quantitative Polymerase Chain Reaction (qPCR) was performed using a LightCycler 480 SYB Green Master Mix (Roche Diagnostics) and real-time PCR RotorGeneQ instrument (Qiagen). PCR conditions were 95 °C for 5 min followed by 40 cycles of 15 s at 95 °C, 10 s at 64 °C and 20 s at 72 °C. Primer sequences were as follows: mRSP9/F: GCT GTT GAC GCT AGA CGA GA, mRSP9/R: ATC TTC AGG CCC AGG ATG TA, mRunx2/F: ACA GTC CCA ACT TCC TGT GC, mRunx2/ R: ACG GTA ACC ACA GTC CCA TC. The levels of Runx2 mRNA were normalized to RSP9 and scaled relative to the expression levels for untreated cells according to the formula  $2^{-\Delta\Delta C_t}$ . Data are shown as the mean of technical duplicates of three *in vitro* experiments.

### 2.9.3. Cancer cells luciferase assay

MDA-MB-231-Luc-RFP cells were seeded at a density of 5000 cells per well in 96-well white opaque tissue culture plates in 200  $\mu$ L phenol red-free F12/ Dulbecco's modified Eagle's medium (DMEM) supplemented with 10 % fetal calf serum (FCS) and incubated for 24 h at 37°C in a humidified atmosphere with 5 % CO<sub>2</sub>. Cells were then washed with PBS



and incubated with PLL/siFLuc or with DHBC-PLL/siFLuc complex formulations at the appropriate N/P ratio (R=1) with the siFLuc concentrations from 50 to 200 nM in OptiMEM at 37°C for 4 h. Thereafter, 50 µL of 40 % serum containing medium was added to reach 10 % of FCS with the final volume of 200 µL. Three days after transfection, expression of luciferase was assessed by addition into culture medium of luciferin ( $10^{-3}$  M, final concentration) purchased from Promega (France). Living cell luminescence was measured 10 min after with a plate reader CLARIOstar® High Performance Monochromator Multimode Microplate Reader (BMG Labtech, Ortenberg, Germany) and averaged from triplicates. The percentage of luminescence of treated cells was calculated by using the control cell as 100 %. Each assay was repeated at least twice. Luciferase activity was normalized in accordance to the total number of living cells in each sample as determined by the MTT assay as previously described (n = 3).

## 2.10. Statistical analysis

R software was used for analysis. Significant differences between two groups were evaluated by a Wilcoxon test. Analysis of variance for more than 2 groups was evaluated with either a Kruskal–Wallis test or an ANOVA when appropriate, followed by a pairwise comparison procedure with a p-value adjustment method of Holm. Values were expressed as the median and inter-quartile range or as mean  $\pm$  SD. Values of  $p < 0.05$  were considered as statistically significant.

## 3. Results and discussion

### 3.1. Synthesis and characterization of PEG-*b*-PCL(COOH) DHBCs

The macromolecular characteristics of the DHBCs (overall molecular weight, length of each block) strongly influence the physical characteristics of the tripartite PCI micelles that may be formed. For example, in the work reported by Raisin *et al.* it was found that the less

asymmetrical copolymer yielded more defined and stable tripartite PIC micelles [24]. We therefore targeted PEG-PCL DHBCs with a similar degree of structural asymmetry in their structure. PEG-*b*-PCL amphiphilic copolymers were first synthesized via the ring-opening polymerization of the CL monomer using PEG as a macroinitiator in the presence of Sn(Oct)<sub>2</sub> as a catalyst. The polymerizations were performed with PEG<sub>43</sub> macroinitiator and predefined amount of CL monomer. The average PCL block length was calculated from the <sup>1</sup>H NMR spectra using the integrals of peaks corresponding to the methylene protons of the CL units and the main chain protons of PEG. A polymerization degree DP = 15 was calculated for the PCL block, corresponding to PEG<sub>43</sub>-*b*-PCL<sub>15</sub> copolymers. The PCL blocks of the copolymers were subsequently functionalized with multiple pendant alkyne groups using the anionic modification methodology reported by our group to yield PEG-*b*-PCL(YNE) [31]. The molecular weight of each block was again calculated based on the <sup>1</sup>H NMR spectrum that confirmed a limited degradation of the PCL block from 1700 g/mol to 1300 g/mol (corresponding to 15 and 12 CL units per chain, respectively). In addition, typical signals of a propargyl group at the α-position of the carbonyl of PCL appeared at 2.0 ppm and between 2.4-2.6 ppm. A degree of substitution of 15 % (DS, number of propargyl groups per 100 CL repeating units corresponding to 2 alkyne groups per PCL block) was calculated by comparing the integral of the signal at 2.4-2.6 ppm with the integral of the PCL methylene signal at 4.1 ppm. The alkyne groups of PEG<sub>43</sub>-*b*-PCL<sub>12</sub>(YNE)<sub>2</sub> were further modified following a fast and efficient thiol-yne photoaddition strategy [29] to introduce the pendant carboxylic groups. The thiol-yne efficiency and carboxylic group content were calculated from the <sup>1</sup>H NMR spectrum of PEG<sub>43</sub>-*b*-PCL<sub>12</sub>(COOH)<sub>6.5</sub> (Figure S2). No peak corresponding to alkene was observed, suggesting that the propargyl groups reacted with two equivalents of thiol and formed only the di-addition product. Peaks are visible in the region from 2.4 to 3.0 ppm which corresponds to the protons of the mercaptosuccinic acid. By comparing the

integral of these peaks with that of the peak at 4.1 ppm corresponding to the methylene protons of PCL, a DS of 25 % of mercaptosuccinic groups with respect to CL was calculated, which corresponds to 50 % of carboxylic acid groups with respect to CL units. Titration of the carboxylic groups confirmed this value with 55 % of carboxylic acid groups with respect to CL units (not shown), which corresponds to ~ 6.5 carboxylic groups per PCL chain. SEC analyses showed a molecular weight increase from  $M_n = 4200$  g/mol for PEG<sub>43</sub>-*b*-PCL<sub>12</sub>(YNE)<sub>2</sub> to  $M_n = 4600$  g/mol for PEG<sub>43</sub>-*b*-PCL<sub>12</sub>(COOH)<sub>6.5</sub> (Figure S3).

### 3.2. Tripartite PIC micelles formulation and loading

#### 3.2.1. Physico-chemical characterization

Tripartite PIC micelles were prepared by mixing the DHBC PEG<sub>43</sub>-*b*-PCL<sub>12</sub>(COOH)<sub>6.5</sub> with PLL and siRNA. In a first step, the characteristics of blank PIC micelles, without the siRNA, were studied by mixing only the DHBC with the PLL at various charge ratios R in PBS (pH 7.4). For R=0.5, *ie.* with a default of cationic groups, the polydispersity index was high (PDI =  $0.472 \pm 0.008$ ) (Figure 1A) in comparison to the other formulations. This higher PDI value can originate from the presence of two size populations detected in DLS, with respective maxima centered on  $D_h = 267 \pm 13$  nm and  $D_h = 52 \pm 3$  nm. The coexistence of these two populations could suggest an incomplete complexation of the polyelectrolytes that results from a lack of PLL positive charges with respect to the negative charges of the DHBC at this particular value of R=0.5. This hypothesis is confirmed considering a 65% decrease of the DCR value for R = 0.5 compared to R = 1 (Figure S8). By increasing the ratio to 1 the PDI decrease to  $0.285 \pm 0.051$  and a single population was observed in DLS with  $D_h = 219 \pm 34$  nm (Figure 1A, 1B). With a further increase of charge ratio to a value of R = 2, larger and more dispersed PIC micelles were again obtained ( $D_h = 255 \pm 48$  nm; PDI =  $0.358 \pm 0.064$ ), which confirms that a charge ratio of 1 is most appropriate for micelle complexation.

Moreover, the zeta potentials of the micelles were studied as a function of R in water (Figure 1C). Results showed, as expected, that the zeta potentials of the blank PIC micelles increased with increasing R values due to the positive charges of PLL. In more details, with R values of 0.5, 1, 2 and 3, the zeta potential varied from  $\xi = -4.9$  mV to 4.4 mV, 13 mV and 20 mV, respectively.

For the rest of the study, we selected a charge ratio of R=1 because of the well-defined PIC micelles obtained in these conditions (single population and lower PDI) and slightly positive zeta potentials of about 4.5 mV. We first investigated the effect of siRNA concentration (1.5  $\mu$ M, 3  $\mu$ M) on the formation and properties of the tripartite PIC micelles. It is to note that the concentration of negative charges brought by siRNA in the formulation (*i.e.*  $6 \times 10^{-5}$  mol/L range for 1.5  $\mu$ M) is negligible compared with  $\sim 2 \times 10^{-3}$  mol/L of respectively negative and positive charges from the DHBC and PLL. The hydrodynamic diameter and the polydispersity index of the micelles were evaluated in PBS (Figure 1D,1E,1F). Introducing siRNA to form the tripartite PIC micelles led to a non-significant decrease of the size and of the polydispersity compared to the blank micelles (Figure 1D, 1E). The trend observed when increasing the concentration of siRNA from 1.5  $\mu$ M to 3  $\mu$ M was a limited increase of the PIC micelles size from  $198 \pm 32$  nm to  $218 \pm 23$  nm ( $219 \pm 34$  nm for blank PIC micelles), along with a limited decrease of PDI from  $0.262 \pm 0.05$  to  $0.235 \pm 0.03$  ( $0.285 \pm 0.051$  for blank PIC micelles). The derived count rate (DCR), which represents the intensity of light scattered by the objects in suspension, was  $170,890 \pm 38,000$  kcps and  $197,000 \pm 9,300$  kcps for these concentrations of siRNA, respectively (Figure 1F). The DCR mostly depends on the size and the concentration of objects in suspension. The slightly higher DCR measured for a siRNA concentration of 3  $\mu$ M can therefore be attributed to the 10 % larger diameters of the PIC micelles obtained under these conditions.

The size of the micelles was further investigated using NTA that confirmed similar sizes for

the blank PIC micelles (B Micelles), polyplexes formed by PLL/siRNA (PLL), as well as siRNA loaded tripartite micelles (Micelles) (Figure S4A). It is important to note that PLL concentrations used here were adjusted to have a concentration similar to the one used in PIC micelles formulation. In these proportions, mixing PLL alone with siRNA led to nanoparticle concentration of  $5.4 \times 10^6$  NP/mL. By contrast, when PLL was mixed with DHBC polymer and siRNA (forming tripartite PIC Micelles), the NP concentration was 100 fold superior ( $4.9 \times 10^8$  NP/mL) (Fig S4B). Interestingly, blank PIC micelles (DHBC/PLL polymers without siRNA), led to the formation of  $3.6 \times 10^8$  NP/mL (Fig S4B).

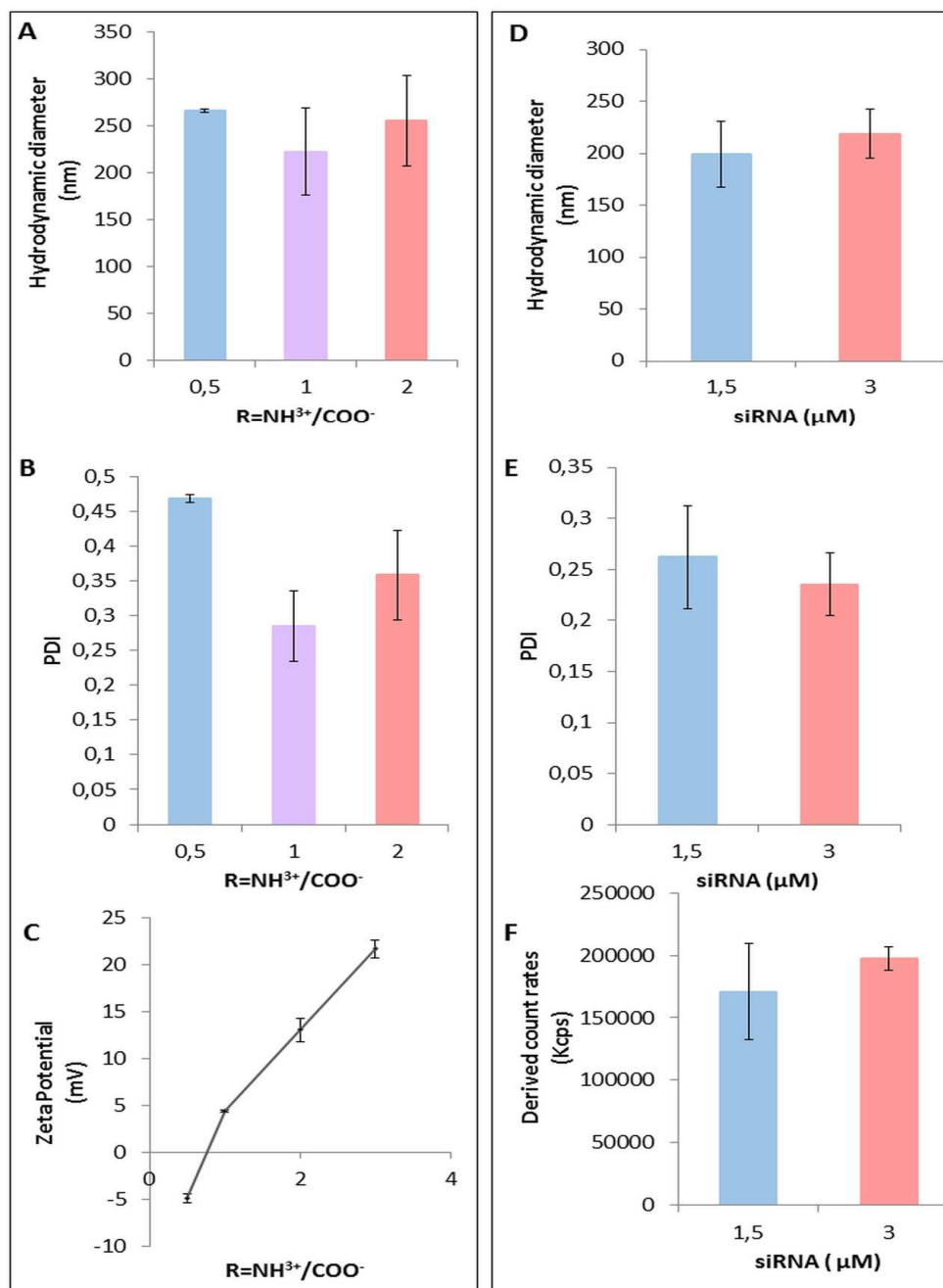


**Figure 1. Characterization of blank and siRNA loaded micelles.** Left: characterization of blank micelles as a function of the charge ratio R with (A) hydrodynamic diameter (Intensity distribution) in PBS; (B) polydispersity index in PBS; (C) zeta potential in water (results correspond to mean  $\pm$  SD, n=3). Right: characterization of siRNA loaded micelles as a function of siRNA concentration in PBS for R=1 with (D) hydrodynamic diameter; (E) polydispersity index; (F) derived count rates (results correspond to mean  $\pm$  SD, n=3).

### 3.2.2. pH-Triggered disassembly

The pH at which PIC micelles disassemble under acidic conditions is mostly determined by the pKa of the polyester carboxylic groups. A pKa of approximately 6 was determined for PEG<sub>43</sub>-*b*-PCL<sub>12</sub>(COOH)<sub>6.5</sub> [28]. For this pKa value, 96 % of the functional groups are under the carboxylate form at pH 7.4, vs. 9 % at pH 5. On the other hand, for the PLL that has a pKa~10, 99.8 % of the functional groups are under the ammonium form at pH 7.4, vs. 100 % at pH 5. We can therefore consider that there is 0.96 anionic charge for 1 cationic charge at pH 7.4, in close accordance with R = 1. On the opposite, at pH 5 there should be less than 0.1 anionic charge for 1 cationic charge. PIC micelles disassembly should therefore be triggered at acidic endosomal pH [32].

In our case, the pH-triggered disassembly was thus assessed by DLS by measuring the derived count rate (DCR) of micellar solutions in PBS at pH 7.4 and pH 5. The formulation with siRNA at a concentration of 3 $\mu$ M was chosen for this study because of its low polydispersity index and its high DCR at pH 7.4. The DCR was significantly lower at pH 5 (61226  $\pm$  10360 kcps) compared to the DCR value at pH 7.4 (197000  $\pm$  9300kcps) (Figure 2A). The high value of the scattered light intensity, and therefore of the DCR, reflects the formation of polymer aggregates of high molecular weight and was previously related to the formation of micelles [33]. In the same pH interval, an increase of the PDI from 0.235  $\pm$  0.030 at pH 7.4, to 0.412  $\pm$  0.072 at pH = 5 was observed (Figure 2B), which can be attributed to a shift from a unimodal to a multimodal population of polydisperse scattering objects.

Beside micelles disassembly, the effective release of RNA from the micelles was evaluated using a spectrofluorimetric assay based on the fluorescence triggered by the Alexa<sub>488</sub>-siRNA. Assuming that RNA molecules trapped inside the micelles are less prone to fluorescence emission, the twice higher fluorescence intensity at pH 5.0 compared to pH 7.4 reported in

Figure 2C suggests that RNA is efficiently released at acidic pH following micelle disassembly.

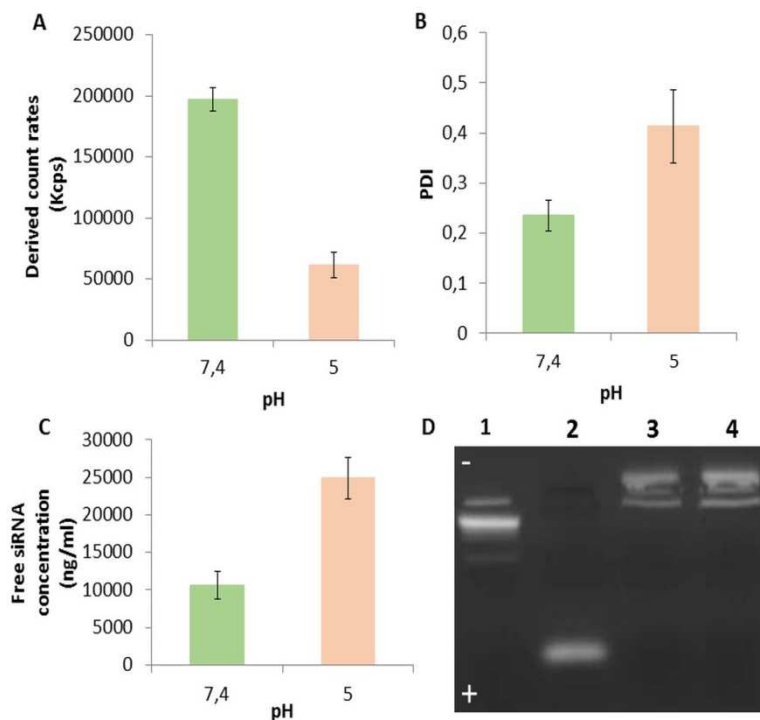


**Figure 2. pH responsiveness of tripartite micelles** with (A) polydispersity index of micelles formed in PBS as a function of pH variation (results correspond to mean  $\pm$  SD, n=3).; (B) derived count rates of micelles in PBS as a function of pH variation (results correspond to mean  $\pm$  SD, n=3); evaluation of siRNA complexation efficiency and pH triggered release with (C) determination of the concentration of siRNA titrated using the fluorescence of Alexa<sub>488</sub>-siRNA, in the presence of PIC micelles in neutral (pH 7.4) and acidic (pH 5) in PBS media (results correspond to mean  $\pm$  SD, n=3); (D) free Alexa<sub>488</sub>-siRNA and Alexa<sub>488</sub>-siRNA complexed within the micelles were loaded in a 5 % agarose electrophoresis gel, molecular weight size markers (line 1); Free siRNA 3  $\mu$ M (line2); PLL with siRNA 3  $\mu$ M R = 1 (line 3); siRNA 3  $\mu$ M complexed with the micelles (line 4).

### 3.2.3. siRNA complexation efficiency



Alexa488-tagged siRNA, free or complexed with the micelles at a concentration of 3  $\mu$ M was loaded at the top of an electrophoresis gel (Figure 2D). Free siRNA migrated slightly toward the cathode due to its negative charge. In contrast, siRNA complexed in tripartite micelles slightly migrated to the anode, probably due to their small excess of positive charges. Moreover, back titration with fluorescently labeled siRNA was performed for the quantitative evaluation of siRNA complexation at pH 7.4. To this purpose, free siRNA was quantified in filtrates after separation from the intact micelles with a 100 kDa Vivaspin<sup>TM</sup> membrane (Figure S5). This allowed us to determine indirectly the siRNA encapsulation rate, which was found equal to 75.7 %. This value is high enough to further consider to use of this system, however, one should note that it is lower than the one reported with the non-degradable DHBC PEO<sub>3k</sub>-*b*-PMAA<sub>1.2k</sub> (encapsulation rate of 93.4 %) [24]. This difference might be attributed to both the charge density of the polymers that is lower for the PEG<sub>43</sub>-*b*-PCL<sub>12</sub>(COOH)<sub>6.5</sub> (55 % of carboxylic groups with respect to CL units *vs.* 100 % with respect to MAA units) and the proximity of the carboxylic groups to the backbone (closer in PMAA than in PCL(COOH)), which result in looser self-assemblies (as shown by large  $D_h$ ) in our case.

Overall, the tripartite PIC micelles show an efficient encapsulation rate of siRNA, a stable complexation at pH 7.4, and a pH-triggered release at acidic pH 5. This set of positive results led us to evaluate the interactions of the tripartite PIC micelles with MSC in terms of cells compatibility, internalization and inhibition of targeted genes.

### 3.3. In vitro evaluation of the potential of the tripartite PIC micelles

#### 3.3.1. Cell viability

The influence of the treatment with the DHBC alone or DHBC/PLL PIC micelles (R=1) on the viability of mMSC was evaluated by an MTS assay (Figure 3A). Concentrations are

calculated in weight of all micelles compounds concentration (PLL, DHBC). It is important to note that DHBC concentrations used here were adjusted to have a concentration similar to the one used in DHBC/PLL PIC micelles formulation. Incubation of cells (48 h) with the DHBC copolymer did not exhibit significant cytotoxicity at all concentration rates with less than 10 % of cell death. Similarly, cell viability was also unaffected upon treatment with DHBC/PLL PIC micelles, up to a concentration of 40  $\mu\text{g/mL}$ . By contrast, cell viability started decreasing with increasing concentrations of DHBC/PLL PIC micelles (R=1) from a concentration of 75  $\mu\text{g/mL}$  and beyond. This result is consistent with the well-documented toxicity of cationic polymers, like PLL at high concentrations [34]. Similar results were obtained with the MDA-MB-231 cancer cells (Figure S7). We therefore concluded that micelles could be safely applied to cells up to a concentration of 40  $\mu\text{g/mL}$ .

### 3.3.2. Internalization efficiency

Micelles internalization into mMSC was quantified by tracking Alexa488 fluorescence attached to siRNA by FACS (Figure 3B). Lipoplexes formulated with lipofectamine2000<sup>®</sup>, used as positive commercial control, yielded the highest internalization compared to the PLL/siRNA polyplexes or the siRNA loaded tripartite PIC micelles (Figure S6). Nevertheless, the fluorescence intensity measured in mMSC was 3 times higher using tripartite PIC micelles compared to PLL/siRNA polyplexes, thus confirming higher extent of internalization provided by our system compared to PLL polyplexes. Incubation of cells with micelles was also performed at 4 °C to block all non-specific energy-dependent endocytosis mechanisms. At 4 °C, the fluorescence intensity was 8 times lower compared to that at 37 °C. These results confirm that an energy dependent endocytosis is probably responsible for micelles internalization. Previous results obtained with a non-degradable PEG-*b*-PMAA counterpart of the PEG-*b*-PCL(COOH) copolymer used in the present work, indicated that tripartite PIC

micelles were internalized into mMSC by a caveolae/lipid-raft dependent mechanism. It is therefore our hypothesis that the PEG-*b*-PCL(COOH)/PLL PIC micelles enter cells via this route that has often been reported for drug delivery with polymeric micelles presenting a PEG corona [35,36].

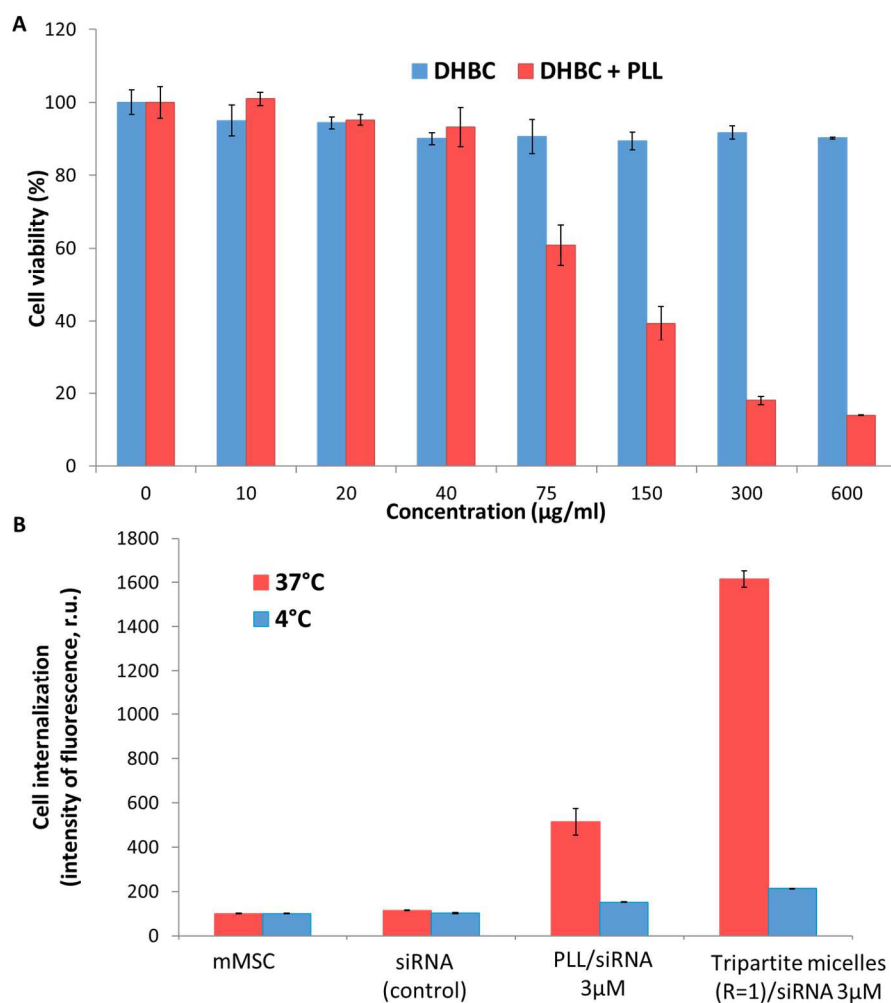


**Figure 3. Evaluation of the micelles cytocompatibility and micelles uptake by mMSC** with (A) cell viability after 48 h of incubation with the DHBC or with DHBC/PLL(R=1) at various dilutions (%), normalized vs. non treated cells, n = 3); (B) internalization of fluorescently labeled non-targeting siRNA (Alexa<sub>488</sub>-siRNA at a concentration of 3µM) in mMSC after 2h at 37°C or 4°C (n=3).

### 3.3.3. Inhibition of a targeted gene expression

The runt related transcription factor (Runx2), which was a targeted gene previously shown to be expressed in MSC and related to bone differentiation, was used for the quantification of extinction of a specific gene expression [37]. We studied the level of mRNA by real-time quantitative PCR to evaluate if our micelles suppress Runx2 expression in the mMSC at a 50 nM Runx2 siRNA concentration (Figure 4A). No decrease in Runx2 expression was observed neither for the tripartite PIC micelles nor for the PLL, which indicates the absence of inhibition in Runx2 expression for these two types of polyplexes.

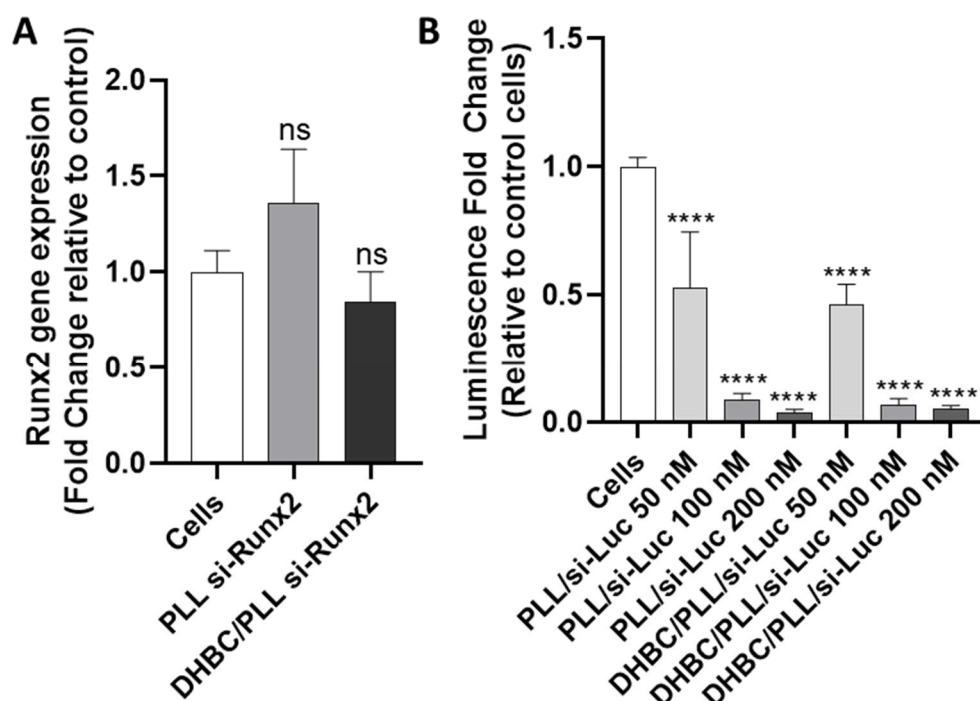


**Figure 4. Inhibition of a target gene expression.** (A) Evaluation of Runx2 silencing. Runx2 mRNA levels for mMSC cells treated with Runx2 siRNA (50 nM) vectorized by tripartite PIC micelles (DHBC/PLL si-Runx2) or PLL (PLL si-Runx2) compared with untreated cells (Cells) (results correspond to mean  $\pm$  SD, n=3). (B) Evaluation of Luciferase silencing. The percentage of luminescence for MDA-MB-231-Luc-RFP cells treated with siFluc vectorized by tripartite PIC micelles (DHBC/PLL si-Luc) or PLL (PLL si-Luc) compared with untreated

cells (Cells) for si-Luc concentrations of 50, 100 and 200 nM (results correspond to mean  $\pm$  SD, n=3). (\*  $p < 0.05$  and \*\*\*\*  $p < 0.0001$  compared to untreated cells)

The lack of efficiency of the tripartite PIC micelles to down-regulate Runx2 expression in mMSC may be related to their incapacity to promote effective endosomal membrane destabilization, which would limit the endosomal escape of the micelles to promote an efficient gene repression. This was not the case for the tripartite PIC micelles formulated with the non-degradable PEG-*b*-PMAA counterpart that led to a 0.38-fold decrease in Runx2 expression and was able to promote endosomal escape due to the well documented ability of PMAA to interact with endosomal membranes [38].

To further investigate this aspect, the ability of the tripartite PIC micelles to inhibit gene expression was tested towards human breast cancer MDA-MB-231-Luc-RFP cells. Formulations were similar to the ones used with mMSCs with exception of the Runx2-targeting siRNA that was replaced by firefly luciferase-targeting siRNA. Gene inhibition was obtained with the tripartite micelles formulations at levels similar (up to ~95 %) to those obtained with PLL polyplexes (Figure 4B). Concentration dependence was witnessed with a decrease of luciferase luminescence with increasing si-Luc concentrations with a significant gene inhibition already obtained at 50 nM of si-Luc, which was not the case with mMSC under the same conditions. This result confirms the ability of degradable DHBC-based tripartite micelles to be internalized into cancer cells, to escape endosomes and release their siRNA payload in the cytoplasm. Further tests should be performed to elucidate why the inhibition of gene expression was efficient with cancer cells but not with mMSCs. Nevertheless, mMSC, as primary cells, are well known as difficult to transfect [39–41] and such studies are beyond the scope of the present work which overall demonstrates that the

degradable PEG-*b*-PCL(COOH) DHBC can constitute a valid alternative to the non-degradable and/or cytotoxic polycation classically used for cell transfection.

#### 4. Conclusion

On the basis of our previous work reporting an efficient chemical strategy to yield novel degradable double hydrophilic block copolymers (DHBCs) [28], we selected in this work the copolymer PEG<sub>43</sub>-*b*-PCL<sub>12</sub>(COOH)<sub>6.5</sub> that combines a non-ionic and bioeliminable PEG block with a carboxylic acid-functionalized PCL block to formulate an original vector for siRNA. We hypothesized that this copolymer could improve the current arsenal of gene therapy vectors that relies mainly on non-degradable and or toxic polymers. The DHBC PEG<sub>43</sub>-*b*-PCL<sub>12</sub>(COOH)<sub>6.5</sub> was prepared in only 3 steps which makes it easily producible compared to the rare examples of degradable DHBCs reported so far for pDNA delivery [26,27]. The results showed that DHBC/PLL/siRNA tripartite PIC micelles with optimized physico-chemical properties ( $D_h \sim 218$  nm, PDI  $\sim 0.235$ ) were able to complex 75 % of siRNA at a charge ratio  $R = 1$ . Under the selected conditions, siRNA was well complexed within the tripartite PIC micelles as shown by electrophoresis and free siRNA evaluation. Interestingly, we evidenced that the tripartite PIC micelles have a pH-stimuli responsive release as the dissociation of the micelles and the release of the siRNA were observed when decreasing the pH from 7.4 to 5. Moreover, results proved that the tripartite PIC micelles had low cytotoxicity and allowed a 3 times higher internalization of siRNA compared to PLL polyplexes in MSCs. Their ability to efficiently inhibit gene expression was found to be dependent on the cells to be transfected with up to 95 % inhibition in MDA-MB-231 cancer cells. Further studies aiming at fine tuning the design (*eg.* charge density) of this class of DHBC to improve the outcome of the tripartite PIC micelles with MSCs will be undertaken,

as we believe that these results will help in the future design of efficient, non-cytotoxic and degradable polymeric vectors for siRNA delivery to mesenchymal stem cells and cancer cells.

**Supplementary Materials:** The following are available online: detailed synthetic procedures for the synthesis of PEG-*b*-PCL based DHBCs; Figure S1: Reaction scheme for the synthesis of the of PEG-*b*-PCL(COOH) DHBCs; Figure S2: <sup>1</sup>H NMR (CDCl<sub>3</sub>) analysis of PEG<sub>43</sub>-*b*-PCL<sub>12</sub>(COOH)<sub>6,5</sub>; Figure S3: Comparative SEC analyses of PEG<sub>43</sub>-*b*-PCL<sub>15</sub>, PEG<sub>43</sub>-*b*-PCL<sub>12</sub>(YNE)<sub>2</sub>, and PEG<sub>43</sub>-*b*-PCL<sub>12</sub>(COOH)<sub>6,5</sub>; Figure S4. Nanoparticle tracking analysis (NTA). Mean size of (A) PLL complexes (PLL) or blank micelles (DHBC/PLL) a charge ratio 0.5, 1 and 2. and (B) PLL polyplexes complexing 3 μM siRNA (PLL siRNA 3 μM) or DHBC micelles complexing siRNA 3 μM (DHBC siRNA 3 μM). Concentrations of (C) PLL complexes (PLL) or blank micelles (DHBC/PLL) a charge ratio 0.5,1 and 2. and (D) PLL polyplexes complexing 3 μM siRNA (PLL siRNA 3 μM) or DHBC micelles complexing siRNA 3 μM (DHBC siRNA 3 μM). determined by nanoparticle tracking analysis (NTA); Figure S5: Schematic protocol for the quantitative determination of the siRNA encapsulation rate in the micelles after separation of free Alexa fluor488-siRNA. Figure S6: Fluorescently labeled non-targeting siRNA (Alexa Fluor 488-siRNA) internalization in mMSC after 2h at 37°C or 4°C. Percent cell internalization was normalized to untreated cells (n=3). Figure S7: Evaluation of the micelles cytocompatibility with MDA-MB-231 cells after 72 h of incubation with DHBC/PLL(R=1) at various dilutions (% , normalized vs. non treated cells, n = 3). Figure S8 : Derived count rates of tripartite PIC micelles at R =0.5 and R = 1 (siRNA 3 μM) compared to derived count rates of PLL/siRNA solutions. Table S1: Typical formulations of tripartite PIC micelles used for physico-chemical analyses

**CRedit author statement:** **Ayman El Jundi:** Investigation, Writing-original draft. **Audrey Bethry:** Investigation. **Jade Berthelot :** Investigation. **Nadir Bettache:** Investigation, Writing-original draft. **Sylvie Hunger:** Investigation. **Jérémy Salvador:** Investigation. **Marie Morille :** Conceptualization, Writing-original draft, Writing - Review & Editing Supervision. **Youssef Bakkour:** Supervision, Funding acquisition. **Emmanuel Belamie:**

Conceptualization, Supervision, Writing - Review & Editing. **Benjamin Nottelet:** Conceptualization, Writing-original draft, Writing - Review & Editing, Funding acquisition, Supervision, Project administration.

**Funding:** This work was partly supported by Research program at the Lebanese University and Lebanese Association for Scientific Research (LASeR).

**Conflicts of Interest:** The authors declare that there is no conflict of interest and are responsible for the content and writing of the article.

#### **References:**

- [1] D. Senapati, B.C. Patra, A. Kar, D.S. Chini, S. Ghosh, S. Patra, M. Bhattacharya, Promising approaches of small interfering RNAs (siRNAs) mediated cancer gene therapy, *Gene*. 719 (2019) 144071. <https://doi.org/10.1016/j.gene.2019.144071>.
- [2] F. Mottaghitalab, A. Rastegari, M. Farokhi, R. Dinarvand, H. Hosseinkhani, K.-L. Ou, D.W. Pack, C. Mao, M. Dinarvand, Y. Fatahi, F. Atyabi, Prospects of siRNA applications in regenerative medicine, *Int. J. Pharm.* 524 (2017) 312–329. <https://doi.org/10.1016/j.ijpharm.2017.03.092>.
- [3] M. Monaghan, A. Pandit, RNA interference therapy via functionalized scaffolds, *Adv. Drug Deliv. Rev.* 63 (2011) 197–208. <https://doi.org/10.1016/j.addr.2011.01.006>.
- [4] X. Zhang, W. Godbey, Viral vectors for gene delivery in tissue engineering☆, *Adv. Drug Deliv. Rev.* 58 (2006) 515–534. <https://doi.org/10.1016/j.addr.2006.03.006>.
- [5] M.A. Kay, J.C. Glorioso, L. Naldini, Viral vectors for gene therapy: the art of turning infectious agents into vehicles of therapeutics, *Nat. Med.* 7 (2001) 33–40. <https://doi.org/10.1038/83324>.
- [6] C.E. Thomas, A. Ehrhardt, M.A. Kay, Progress and problems with the use of viral vectors for gene therapy, *Nat. Rev. Genet.* 4 (2003) 346–358. <https://doi.org/10.1038/nrg1066>.
- [7] J.M. McMahon, S. Conroy, M. Lyons, U. Greiser, C. O'shea, P. Strappe, L. Howard, M. Murphy, F. Barry, T. O'brien, Gene Transfer into Rat Mesenchymal Stem Cells: A



- Comparative Study of Viral and Nonviral Vectors, *Stem Cells Dev.* 15 (2006) 87–96. <https://doi.org/10.1089/scd.2006.15.87>.
- [8] A.R. Sousa, A.V. Oliveira, M.J. Oliveira, B. Sarmento, Nanotechnology-based siRNA delivery strategies for metastatic colorectal cancer therapy, *Int. J. Pharm.* 568 (2019) 118530. <https://doi.org/10.1016/j.ijpharm.2019.118530>.
- [9] X. Zhao, D.-C. Li, H. Zhao, Z. Li, J.-X. Wang, D.-M. Zhu, J. Zhou, J.-N. Cen, A study of the suppressive effect on human pancreatic adenocarcinoma cell proliferation and angiogenesis by stable plasmid-based siRNA silencing of c-Src gene expression, *Oncol. Rep.* (2011). <https://doi.org/10.3892/or.2011.1602>.
- [10] J. Hoelters, M. Ciccarella, M. Drechsel, C. Geissler, H. Gülkan, W. Böcker, M. Schieker, M. Jochum, P. Neth, Nonviral genetic modification mediates effective transgene expression and functional RNA interference in human mesenchymal stem cells, *J. Gene Med.* 7 (2005) 718–728. <https://doi.org/10.1002/jgm.731>.
- [11] S. Elsler, S. Schetting, G. Schmitt, D. Kohn, H. Madry, M. Cucchiari, Effective, safe nonviral gene transfer to preserve the chondrogenic differentiation potential of human mesenchymal stem cells: Nonviral vectors for hMSC chondrogenesis, *J. Gene Med.* 14 (2012) 501–511. <https://doi.org/10.1002/jgm.2644>.
- [12] C.R. Dass, Cytotoxicity issues pertinent to lipoplex-mediated gene therapy in-vivo, *J. Pharm. Pharmacol.* 54 (2002) 593–601. <https://doi.org/10.1211/0022357021778817>.
- [13] R.H. Mo, J.L. Zaro, J.-H.J. Ou, W.-C. Shen, Effects of Lipofectamine 2000/siRNA Complexes on Autophagy in Hepatoma Cells, *Mol. Biotechnol.* 51 (2012) 1–8. <https://doi.org/10.1007/s12033-011-9422-6>.
- [14] L.-L. Farrell, J. Pepin, C. Kucharski, X. Lin, Z. Xu, H. Uludag, A comparison of the effectiveness of cationic polymers poly-l-lysine (PLL) and polyethylenimine (PEI) for non-viral delivery of plasmid DNA to bone marrow stromal cells (BMSC), *Eur. J. Pharm. Biopharm.* 65 (2007) 388–397. <https://doi.org/10.1016/j.ejpb.2006.11.026>.
- [15] B.A. Clements, V. Incani, C. Kucharski, A. Lavasanifar, B. Ritchie, H. Uludağ, A comparative evaluation of poly-l-lysine-palmitic acid and Lipofectamine™ 2000 for plasmid delivery to bone marrow stromal cells, *Biomaterials.* 28 (2007) 4693–4704. <https://doi.org/10.1016/j.biomaterials.2007.07.023>.
- [16] M.L. Patil, M. Zhang, O. Taratula, O.B. Garbuzenko, H. He, T. Minko, Internally Cationic Polyamidoamine PAMAM-OH Dendrimers for siRNA Delivery: Effect of the Degree of Quaternization and Cancer Targeting, *Biomacromolecules.* 10 (2009) 258–266. <https://doi.org/10.1021/bm8009973>.

- [17] J. Zhao, G. Weng, J. Li, J. Zhu, J. Zhao, Polyester-based nanoparticles for nucleic acid delivery, *Mater. Sci. Eng. C*. 92 (2018) 983–994.  
<https://doi.org/10.1016/j.msec.2018.07.027>.
- [18] C. Fu, X. Sun, D. Liu, Z. Chen, Z. Lu, N. Zhang, Biodegradable Tri-Block Copolymer Poly(lactic acid)-poly(ethylene glycol)-poly(L-lysine)(PLA-PEG-PLL) as a Non-Viral Vector to Enhance Gene Transfection, *Int. J. Mol. Sci.* 12 (2011) 1371–1388.  
<https://doi.org/10.3390/ijms12021371>.
- [19] C. He, Z. Zhang, Q. Yang, Q. Chang, Z. Shao, B. Gong, Y.-M. Shen, B. Liu, Z. Zhu, Reductive triblock copolymer micelles with a dynamic covalent linkage deliver anti-miR-21 for gastric cancer therapy, *Polym. Chem.* 7 (2016) 4352–4366.  
<https://doi.org/10.1039/C6PY00651E>.
- [20] K.A. Woodrow, Y. Cu, C.J. Booth, J.K. Saucier-Sawyer, M.J. Wood, W. Mark Saltzman, Intravaginal gene silencing using biodegradable polymer nanoparticles densely loaded with small-interfering RNA, *Nat. Mater.* 8 (2009) 526–533.  
<https://doi.org/10.1038/nmat2444>.
- [21] O.M. Merkel, A. Beyerle, D. Librizzi, A. Pfestroff, T.M. Behr, B. Sproat, P.J. Barth, T. Kissel, Nonviral siRNA Delivery to the Lung: Investigation of PEG–PEI Polyplexes and Their In Vivo Performance, *Mol. Pharm.* 6 (2009) 1246–1260.  
<https://doi.org/10.1021/mp900107v>.
- [22] I.K. Voets, A. de Keizer, M.A. Cohen Stuart, Complex coacervate core micelles, *Adv. Colloid Interface Sci.* 147–148 (2009) 300–318.  
<https://doi.org/10.1016/j.cis.2008.09.012>.
- [23] A.E. Felber, B. Castagner, M. Elsbahy, G.F. Deleavey, M.J. Damha, J.-C. Leroux, siRNA nanocarriers based on methacrylic acid copolymers, *J. Controlled Release*. 152 (2011) 159–167. <https://doi.org/10.1016/j.jconrel.2010.12.012>.
- [24] S. Raisin, M. Morille, C. Bony, D. Noël, J.-M. Devoisselle, E. Belamie, Tripartite polyionic complex (PIC) micelles as non-viral vectors for mesenchymal stem cell siRNA transfection, *Biomater. Sci.* 5 (2017) 1910–1921. <https://doi.org/10.1039/C7BM00384F>.
- [25] M.J. Geisow, W.H. Evans, pH in the endosome, *Exp. Cell Res.* 150 (1984) 36–46.  
[https://doi.org/10.1016/0014-4827\(84\)90699-2](https://doi.org/10.1016/0014-4827(84)90699-2).
- [26] P. Zhang, Z. Zhang, Y. Yang, Y. Li, Folate-PEG modified poly(2-(2-aminoethoxy)ethoxy)phosphazene/DNA nanoparticles for gene delivery: Synthesis, preparation and in vitro transfection efficiency, *Int. J. Pharm.* 392 (2010) 241–248.  
<https://doi.org/10.1016/j.ijpharm.2010.03.030>.

- [27] S. Takae, K. Miyata, M. Oba, T. Ishii, N. Nishiyama, K. Itaka, Y. Yamasaki, H. Koyama, K. Kataoka, PEG-Detachable Polyplex Micelles Based on Disulfide-Linked Block Cationomers as Bioresponsive Nonviral Gene Vectors, *J. Am. Chem. Soc.* 130 (2008) 6001–6009. <https://doi.org/10.1021/ja800336v>.
- [28] A. El Jundi, S. Buwalda, A. Bethry, S. Hunger, J. Coudane, Y. Bakkour, B. Nottelet, Double-Hydrophilic Block Copolymers Based on Functional Poly( $\epsilon$ -caprolactone)s for pH-Dependent Controlled Drug Delivery, *Biomacromolecules*. 21 (2020) 397–407. <https://doi.org/10.1021/acs.biomac.9b01006>.
- [29] A. Al Samad, Y. Bakkour, C. Fanny, F. El Omar, J. Coudane, B. Nottelet, From nanospheres to micelles: simple control of PCL-g-PEG copolymers' amphiphilicity through thiol-yne photografting, *Polym. Chem.* 6 (2015) 5093–5102.
- [30] N. Mebarek, R. Vicente, A. Aubert-Pouëssel, J. Quentin, A.-L. Mausset-Bonnefont, J.-M. Devoisselle, C. Jorgensen, S. Bégu, P. Louis-Pence, Versatile polyion complex micelles for peptide and siRNA vectorization to engineer tolerogenic dendritic cells, *Eur. J. Pharm. Biopharm.* 92 (2015) 216–227. <https://doi.org/10.1016/j.ejpb.2015.03.013>.
- [31] S. Buwalda, A. Al Samad, A. El Jundi, A. Bethry, Y. Bakkour, J. Coudane, B. Nottelet, Stabilization of poly(ethylene glycol)-poly( $\epsilon$ -caprolactone) star block copolymer micelles via aromatic groups for improved drug delivery properties, *J. Colloid Interface Sci.* 514 (2018) 468–478. <https://doi.org/10.1016/j.jcis.2017.12.057>.
- [32] J. Huotari, A. Helenius, Endosome maturation: Endosome maturation, *EMBO J.* 30 (2011) 3481–3500. <https://doi.org/10.1038/emboj.2011.286>.
- [33] J. Reboul, T. Nugay, N. Anik, H. Cottet, V. Ponsinet, M. In, P. Lacroix-Desmazes, C. Gerardin, Synthesis of double hydrophilic block copolymers and induced assembly with oligochitosan for the preparation of polyion complex micelles, *Soft Matter*. 7 (2011) 5836–5846. <https://doi.org/10.1039/c1sm05230f>.
- [34] Z. Kadlecova, L. Baldi, D. Hacker, F.M. Wurm, H.-A. Klok, Comparative Study on the In Vitro Cytotoxicity of Linear, Dendritic, and Hyperbranched Polylysine Analogues, *Biomacromolecules*. 13 (2012) 3127–3137. <https://doi.org/10.1021/bm300930j>.
- [35] Z. Zhang, X. Xiong, J. Wan, L. Xiao, L. Gan, Y. Feng, H. Xu, X. Yang, Cellular uptake and intracellular trafficking of PEG-b-PLA polymeric micelles, *Biomaterials*. 33 (2012) 7233–7240. <https://doi.org/10.1016/j.biomaterials.2012.06.045>.
- [36] G. Sahay, D.Y. Alakhova, A.V. Kabanov, Endocytosis of nanomedicines, *J. Controlled Release*. 145 (2010) 182–195. <https://doi.org/10.1016/j.jconrel.2010.01.036>.

- [37] J. Huang, L. Zhao, L. Xing, D. Chen, MicroRNA-204 Regulates Runx2 Protein Expression and Mesenchymal Progenitor Cell Differentiation, *Stem Cells*. 28 (2010) 357–364. <https://doi.org/10.1002/stem.288>.
- [38] M. Yessine, Membrane-destabilizing polyanions: interaction with lipid bilayers and endosomal escape of biomacromolecules, *Adv. Drug Deliv. Rev.* 56 (2004) 999–1021. <https://doi.org/10.1016/j.addr.2003.10.039>.
- [39] S. Raisin, E. Belamie, M. Morille, Non-viral gene activated matrices for mesenchymal stem cells based tissue engineering of bone and cartilage, *Biomaterials*. 104 (2016) 223–237. <https://doi.org/10.1016/j.biomaterials.2016.07.017>.
- [40] A. Hamm, N. Krott, I. Breibach, R. Blindt, A.K. Bosserhoff, Efficient Transfection Method for Primary Cells, *Tissue Eng.* 8 (2002) 235–245. <https://doi.org/10.1089/107632702753725003>.
- [41] J. L. Santos, D. Pandita, J. Rodrigues, A. P. Pego, P. L. Granja, H. Tomas, Non-Viral Gene Delivery to Mesenchymal Stem Cells: Methods, Strategies and Application in Bone Tissue Engineering and Regeneration, *Curr. Gene Ther.* 11 (2011) 46–57. <https://doi.org/10.2174/156652311794520102>.

